Supporting Information

LeSauter et al. 10.1073/pnas.0906426106

SI Text

Results. *Colocalization of ghrelin and clock proteins in stomach.* Because oxyntic cells of the stomach are the primary source of plasma ghrelin, we assessed whether they bear a molecular circadian clock machinery. The oxyntic gland tissue was harvested from the stomach's corpus region (Fig. S2*A*). The results indicate that ghrelin-containing oxyntic cells express the clock proteins PER1 and PER2 (Fig. S2*B*). At CT18, when PER proteins peak (see below), most ghrelin-containing cells coexpress PER1 (84.0% ± 3.4%) and PER2 (88.5% ± 2.1%).

Rhythms of ghrelin in cells in the stomach of clock mutant mice. We surmised that if the molecular clockwork machinery was mutated, rhythmic ghrelin should be disrupted. Thus, we characterized the pattern of ghrelin expression in *mPer1,mPer2* double-mutant mice that are arrhythmic in constant darkness (1). In wild-type animals, ghrelin expression was higher at CT6 than at CT18 in both ad libitum and food-deprived conditions (Fig. S3*A*). In contrast, there was no difference between these time points in ghrelin expression in the *mPer1,mPer2^{Brdm1}* double mutant. We conclude that a mutation in the circadian clock mechanism abolishes rhythmic expression of ghrelin.

A functional circadian clock is necessary for food anticipatory ghrelin release. Given that the stomach is the source of most of the plasma ghrelin, we used another group of animals to ask whether oxyntic cell ghrelin content decreases as normal before food presentation in animals with a dysfunctional circadian clock. In wild-type mice, but not in *mPer1,Per2^{Brdm1}* double-mutant animals, when food availability is restricted to ZT12–ZT18, expression of ghrelin is decreased just before food presentation, compared with ZT6 (Fig. S3*B*). This suggests that the circadian system times the release of ghrelin. The question of whether clock mutant mice show FAA is not resolved at present. The *Per2^{Brdm1}* mouse maintained on an 8-h food availability schedule does not show FAA (2). The *mPer1,mPer2^{ldc}* mutant (among others) maintained on a 3-h food availability schedule does show FAA (3). The difference among studies may be the result of homeostatic signals resulting from short duration of food availability. It is noteworthy that the mice used in the present study differ from those of Storch and Weitz (3). Given strain differences, as well as the possibility that compensatory mechanisms may emerge in mice with a null mutant allele (as in the *mPer2^{ldc}*) versus those with in-frame deletions (as in the *mPer2^{Brdm1}*) (4), the results of the Storch and Weitz experiment cannot be extrapolated to the animals used here.

Methods. *Transmitter implants: recording of general activity.* Mice were deeply anesthetized with 60 mg/kg ketamine and 5 mg/kg xylazine. A 2-cm midline lower abdominal laparotomy was performed. The transmitter (VM-FH; MiniMitter) was coated with a silicone elastomer outer layer and was inserted into the abdominal cavity, and abdominal muscle and fascia were closed. To monitor general activity, the animals' cages were placed on an RTA-500 telemetry receiver plate (MiniMitter) connected to a computer. An activity event was scored whenever a change in signal strength from the transmitter exceeded a threshold. General activity was recorded in 2-min bins by using Datacol 3 software (MiniMitter)

Expression of ghrelin and clock proteins. To determine whether oxyntic cells contain the circadian clock molecular machinery, the corpus aspect of the stomach was stained for ghrelin and the clock proteins PER1 and PER2 in C57BL/6 mice killed at ZT18 (*n* = 5), a time of high PER protein expression.

To test whether a functional circadian system is necessary for rhythmic ghrelin expression, *mPer1,mPer2* double-mutant mice (*mPer1-mPer2^{Brdm1}* strain) (ref. 1; gift from Zhong Sun; Cornell Weil Medical Center, New York) and control C57BL/6 mice, fed ad libitum, were maintained in a 12:12 LD cycle, and then housed in DD for 42 or 54 h and killed at CTs 6 or 18 (projected from ZT6 or ZT18), respectively (*n* = 4 per group). To assess whether ghrelin, PER1, and PER2 protein rhythms could be entrained by periodic food intake, animals were housed in DD and food-deprived for exactly 24 h before being killed at the projected CT6 and CT18 (*n* = 4 per time point). To test for premeal gastric ghrelin contents, *mPer1,mPer2* double-mutant mice were maintained in an LD 12:12 and fed ZT12–ZT18 for 1 week, and then killed at ZT6 and ZT12.

Perfusion and immunohistochemistry. Animals were deeply anesthetized (200 mg/kg pentobarbital, i.p.). Mice killed in the dark were anesthetized under the dim red light and their heads covered with a light-proof hood until they were perfused. Mice were perfused intracardially with 50 mL of saline followed by 100 mL of 4% paraformaldehyde in 0.1 M phosphate buffer (PB), pH 7.3. Stomachs were postfixed for 18–24 h at 4 °C and cryoprotected in 20% sucrose in 0.1 M PB overnight.

The corpus region of the stomach was dissected and blocked for sectioning. Sections cut on a cryostat (15 μm) were processed on slides. Rhythms in ghrelin, PER1, and PER2 expression were detected in single-labeled sections stained with an avidin–biotin–immunoperoxidase technique using DAB (Sigma) as the chromogen. Colocalization was analyzed in double-labeled sections that were incubated in donkey serum for 1 h, then in ghrelin antibody made in goat (polyclonal; 1:5,000; Santa Cruz Biotechnology) and either PER1 (rabbit polyclonal; 1:8,000; gift from S. M. Reppert and D. R. Weaver, University of Massachusetts, Worcester, MA) or PER2 (mouse monoclonal; 1:5,000; Alpha Diagnostic) for 48 h. After washes, sections were incubated in donkey anti-goat and donkey anti-rabbit (for PER1) or anti-mouse (for PER2) secondary antibodies conjugated to the Cy2 and Cy3 fluorophores (1:200; Jackson ImmunoResearch) for 2 h. Sections were coverslipped with Permount (Fisher Scientific) for DAB or Krystalon (EMD Chemicals) for Cy2 and Cy3.

To test for specificity, sections were stained with fluorescent Cy2 by (*i*) omitting the primary antibodies (ghrelin, PER1, or PER2), or (*ii*) by preincubation with ghrelin (1:500; Santa Cruz Biotechnology) or PER2 peptide (1:500; Alpha Diagnostic), and (*iii*) by staining sections for ghrelin in a ghrelin-knockout mouse (tissue provided by Tamas Horvath) and staining for PER1 and PER2 in *mPer1,mPer2* double-mutant mice. Staining was not detected after omission of primaries. Ghrelin and PER2 staining were eliminated by preincubation. Ghrelin staining was not detected in the ghrelin-knockout mouse, nor was PER1 or PER2 staining detected in *mPer1,mPer2* double-mutant mice. (Fig. S5).

Analysis of immunostaining. Images of gastric sections were captured by using a CCD video camera (Sony XC77) attached to a light microscope (Olympus BH-2) using National Institutes of Health (NIH) Image 1.61. Three sections were analyzed per stomach. Two observers blind to the experimental conditions processed the photographs with NIH Image 1.61 software to provide a quantitative estimate of the number of immunoreactive ghrelin cells. The images were analyzed in grayscale without any adjustment of brightness or contrast. The density slice threshold was adjusted for 1 section and kept constant thereafter. To measure the number of ghrelin cells, the particle size was

adjusted to 100–500 pixels (the size of a ghrelin-expressing cell is ≈150–350 pixels). The "analyze particles" command gave the number of cells in each photograph. Because dense packing of PER1- and PER2-stained oxyntic cells prevented counting of individual cells, the intensity of staining was assessed as relative optical density (ROD) measured as optical density of staining within the region of oxyntic cells minus optical density of background. The staining for each animal was expressed as the average ROD in 3 stomach sections. One-way ANOVA, or t test, was used to test for time of day effects.

Coexpression of ghrelin and PER1 or ghrelin and PER2 was analyzed on confocal optical images. Slides were observed under a Zeiss Axiovert 200 MOT fluorescence microscope (Carl Zeiss) with a Zeiss LSM 410 laser scanning confocal attachment. The sections were excited with an argon-krypton laser using the excitation wavelengths 488 nm for Cy2 and 543 nm for Cy3. The images were collected as 1-μm optical images with sequential excitation by each laser to avoid cross-talk between wavelengths. Each cell was examined in ≈10 sequential optical images to verify that it was double-labeled, by using the LSM 3.95 software (Zeiss) to separate/superimpose green and red. Three stomach sections were analyzed per animal at each time point.

1. Zheng B, et al. (2001) Nonredundant roles of the mPer1 and mPer2 genes in the mammalian circadian clock. *Cell* 105:683–694.
2. Feillet CA, et al. (2006) Lack of food anticipation in Per2 mutant mice. *Curr Biol* 16:2016–2022.
3. Storch KF, Weitz CJ (2009) Daily rhythms of food-anticipatory behavioral activity do not require the known circadian clock. *Proc Natl Acad Sci USA* 106:6808–6813.
4. Takahashi JS, Shimomura K, Kumar V (2008) Searching for genes underlying behavior: Lessons from circadian rhythms. *Science* 322:909–912.
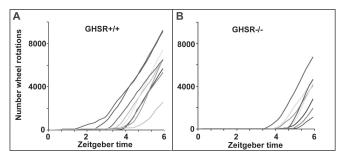
Fig. S1. Cumulative wheel running data for individual GSHR$^{+/+}$ (*A*) and GSHR$^{-/-}$ (*B*) animals. In Fig. 2*C*, the standard errors for group data around each point reflect the differences (shown here) among individual animals in thresholds for initiating activity. The data, averaged over the 7 last days of food restriction, show that once that ''go'' decision is made, the animal continues to run as feeding time approaches.
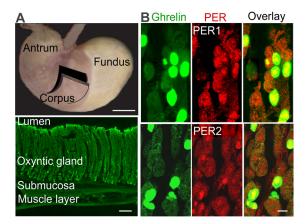
Fig. S2. Low- and high-magnification views of the stomach, oxyntic cells, and localization of ghrelin and PER proteins. (*A*) (*Upper*) Image of the mouse stomach, indicating the corpus region where tissue was harvested. (Scale bar: 500 μm.) (*Lower*) Photomicrograph of a cross-section of the stomach wall. (Scale bar: 100 μm.) (*B*) Photomicrographs of the stomach oxyntic gland stained for ghrelin, PER1 (*Upper*) or PER2 (*Lower*) and the overlay in optical sections (*z* axis = 2 μm). (Scale bar: 10 μm.)
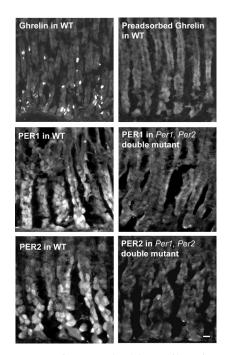
Fig. S3. Photomicrographs of the stomach oxyntic cells stained for ghrelin (CY2) (*Top Left*) or after preincubation with ghrelin peptide (1:500; Santa Cruz Biotechnology) (*Top Right*); PER1 in wild-type (*Middle Left*) and *mPer1,mPer2* double-mutant (*Middle Right*) mice; PER2 in wild-type (*Bottom Left*) and in *mPer1,mPer2* double-mutant (*Bottom Right*) mice. (Scale bar: 20 μm.)
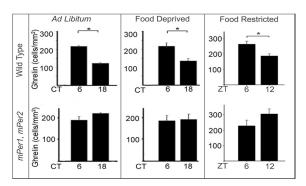
Fig. S4. (*A*) Comparison of ghrelin immunoreactive cells in wild-type and *mPer1,mPer2* clock mutant animals. Number of oxyntic cells expressing ghrelin in animals housed in LD and then placed in DD for 2 days and then either fed ad libitum (*Left*), food-deprived for 24 h (*Middle*), or food-restricted (*Right*; see *Materials and Methods* for details). ∗, $P < 0.05$.
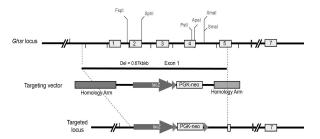
Fig. S5. Generation of ghrelin receptor knockout (GHSR$^{-/-}$) and control GHSR$^{+/+}$ mice (provided by M. W. Sleeman, Regeneron Pharmaceuticals). Bacterial artificial chromosome for *Ghsr* was isolated, and targeting vectors in which exon 1 of the *Ghsr* locus was precisely deleted and replaced with an in-frame lacZ reporter gene and neomycin-selectable marker were electroporated into embryonic stem cells. Correctly targeted embryonic stem cells, as well as eventual heterozygotes and homozygous mice derived from these embryonic stem cells, were identified by a real-time PCR-based loss-of-native-allele assay, as described previously [Valenzuela DM, et al. (2003) *Nat Biotechnol* 21:652–659]. After germ-line transmission was established, F$_1$ heterozygous mice were backcrossed to C57BL6/J to generate N3 breeding heterozygote pairs that were used to generate homozygous *GHSR*$^{+/+}$ and *GHSR*$^{-/-}$ mice used in these experiments. Deletion of *Ghsr* was also confirmed by the absence of exogenous ghrelin-induced feeding response (M. W. Sleeman, Regeneron Pharmaceuticals).